Optics Communications 458 (2020) 124848

Contents lists available at ScienceDirect

Optics Communications

journal homepage: www.elsevier.com/locate/optcom

Predict sample's line positions of absorption peaks in terahertz band with the forced radiation intensity of molecular electric dipoles

Zhongwei Zhang [a,b,*], Zhi Zhu [a], Minghui Yuan [a], Minghui Li [b], Guanjun You [a], Lin Chen [a], Yiming Zhu [a,**]

[a] Terahertz Technology Innovation Research Institute, Shanghai Key Lab of Modern Optical System, Terahertz Science Cooperative Innovation Center, School of Optical-Electrical Computer Engineering, University of Shanghai for Science and Technology, No. 580 Jun Gong Road, Shanghai 200093, China
[b] Department of Optical Engineering, School of Sciences, Zhejiang A&F University, Hangzhou, 311300, Zhejiang Province, China

ARTICLE INFO

Keywords:
Spectrum analysis
Electric dipole
Terahertz (THz)
Water vapor
Coherent superposition
Density functional theory (DFT)

ABSTRACT

Directly predicting the line positions of samples in the terahertz (THz) band is of significant importance for their THz identification. However, it is really a challenge to gain accurately the line positions by means of theoretical calculation, because the calculation typically involves various parameters, such as level energy and transition moment, which usually we hardly get directly. Based on the classical forced vibration model of dipoles, we propose a quantitative expression, i.e. the forced radiation intensity of molecular electric dipoles, which intend to predict the line positions of absorption peaks in the THz fingerprint spectra of a sample. We verified our expression by 9 recognized frequencies selected from the fingerprint spectra of water vapor in the THz band. Both the line positions and intensities of the absorption peaks of water vapor we calculated by the expression are well consistent with the experimental measurements. The line positions we calculated are also more accurate and comprehensive than that of water clusters simulated from Density Functional Theory (DFT). Our findings further support the theory of coherent superposition to advance a new method to exactly analyze the generation mechanism of molecular THz-fingerprint spectroscopy of a sample.

1. Introduction

The terahertz (THz) spectral region is associated with fundamental physical processes such as vibrational motions of organic compounds, and lattice vibrations in solids [1,2]. Compared with radio waves and infrared radiation, the THz band shows exceedingly high atmospheric opacity because the absorption by water vapor is the predominant cause of atmospheric THz attenuation [3,4]. Moreover, water vapor has its own characteristic fingerprint spectra in THz band [5–9], which can be used as a background coordinate reference system for a sample's identification. Therefore, water absorption is an important factor that must be considered when designing an operational scheme for a THz identification.

Usually, fingerprint spectra are widely used to identify samples [10]. The line positions of absorption peaks in a sample's fingerprint spectra correspond to the characteristic frequencies. Although samples also have fingerprint spectra in the infrared region [11], their THz characteristic fingerprint spectra can more accurately imply the structural properties of material molecules. However, three major problems still need to be settled: (1) Except some algorithms, such as DFT, and FFT (Fast Fourier Transform), there has no explicit mathematical expression which can show the characteristic responses of a sample in the THz range. Therefore, it is impossible to verify theoretically whether a central frequency of an absorption peak measured by THz-TDS system is correctly corresponding to the fingerprint frequency of a sample molecule. (2) Components of transmission intensity are complex, and there are no quantitative expressions to define them and compare them with experimental spectra. Su et al. [12] analyzed THz spectral fingerprint identification with improved performance based on empirical mode decomposition, and they conducted experiments on water vapor and carbon monoxide with THz-TDS, respectively. However, it is still difficult to recognize each component of transmission intensity in their experimental spectra. (3) For a molecule with an unknown structure, e.g. organic molecule, it is extremely difficult to predict its line positions of absorption peaks.

Intending to solve these above-mentioned problems, in this paper, we propose a quantitative expression, i.e. the radiation intensity of

* Corresponding author at: Terahertz Technology Innovation Research Institute, Shanghai Key Lab of Modern Optical System, Terahertz Science Cooperative Innovation Center, School of Optical-Electrical Computer Engineering, University of Shanghai for Science and Technology, No. 580 Jun Gong Road, Shanghai 200093, China.
** Corresponding author.
E-mail addresses: free35@163.com (Z. Zhang), ymzhu@usst.edu.cn (Y. Zhu).

https://doi.org/10.1016/j.optcom.2019.124848
Received 31 July 2019; Received in revised form 14 October 2019; Accepted 29 October 2019
Available online 1 November 2019

forced vibration produced by all the molecular electric dipoles irradiated by THz waves, which is derived from the classical forced vibration model of dipoles [13,14]. It can be used to quantitatively calculate the line positions of absorption peaks of a sample molecule. Although some studies have found that it is a challenge in the accurate calculation of line positions, because the calculation usually involves some parameters, such as energy levels and transition moments [15–17], which usually we hardly get directly. Now, the interaction process between THz waves and a sample molecule becomes simple when we only concern the classical forced vibration model of the dipole. The model insists that each molecule in a sample can be regarded as an oscillating electric dipole, whose radiation intensity of forced vibration belongs to the component of transmission intensity, and it carries the characteristic information of the sample.

In the following parts of this paper, we give the derivation of our expression. Then, we use the THz spectra of water vapor to prove it, while taking 9 recognized intrinsic central frequencies of water vapor as an example. We find that both the calculated positions and intensities of absorption peaks by our expression agree perfectly with the experimental results. Next, to verify the superiority of our expression, it is compared with the line positions of water clusters simulated from DFT. The results show that the line positions calculated by our expression are more accurate and comprehensive than that of DFT. So, our study not only contributes to providing a new practical method for predicting and calculating line positions of absorption peaks of simple samples, but paves the way to calculate the characteristic positions of organic molecules and solid plasmonic samples [18] as well. In addition, specially, our expression also supports the theory of coherent superposition to exactly analyze the generation mechanism of fingerprint spectroscopy of molecules at THz frequencies. As far as we know, there are very few studies [19–22] on the coherent superposition in the current field of THz absorption spectroscopy, while our study shows good self-consistency to the coherent superposition in this paper.

2. Forced radiation intensity of molecular electric dipoles in a sample

Traditionally, each molecule in a sample can be regarded as an oscillating electric dipole [13]. Its oscillations produce radiating electromagnetic fields to its surrounding space. If the attenuation is neglected, the oscillations can be taken as a series of simple harmonic vibrations at ω_{0i}, the intrinsic central angular frequency of the ith dipole. Now, we take the vibration direction as x. The vibrating displacement of the ith dipole is $x_i = x_{0i}\exp[-j(\omega_{0i}t+\varphi_i)]$, where φ_i is the initial phase of the dipole. As the vibration time $t = 0$, the incident THz field with electric field amplitude E_0 acts on the dipole at the frequency ω. The electric field intensity of the incident THz wave can be expressed as $E(t) = E_0\exp(-j\omega t)$, where j is the imaginary unit.

When an incident THz wave passes through a sample, the quasi-electron in the ith dipole is forced to vibrate under the driving force of the electric field generated by the incident THz wave [13,14]. We express the motion equation of the quasi-electron as:

$$\frac{d^2x}{dt^2} + \gamma\frac{dx}{dt} + \omega_{0i}^2 x = \frac{eE}{m_i} = \frac{eE_0}{m_i}e^{-j\omega t} \tag{1}$$

where $\gamma = \frac{1}{4\pi\varepsilon_0}\frac{2}{3}\frac{e^2\omega_{0i}^2}{mc^3}$ is the damping coefficient of the THz wave in a sample. ε_0 is the vacuum permittivity, e is the elementary charge, m is the quasi-electron mass of a sample molecule, and c is the speed of light in vacuum. m_i, and ω_{0i} are the mass, the intrinsic central angular frequency of the ith dipole, respectively.

The steady-state solution of Eq. (1) is:

$$x = \frac{eE_0}{m_i}\frac{e^{-j(\omega t+\delta)}}{\sqrt{\left(\omega_{0i}^2-\omega^2\right)^2-(\omega\gamma)^2}} \tag{2}$$

where the phase difference between the forced vibration of quasi-electron and the incident THz field is

$$\delta = \arctan\frac{\omega\gamma}{\omega^2-\omega_{0i}^2} \tag{3}$$

and it is also the phase difference between transmitted THz waves modulated by dipoles' motion. When $\omega = \omega_{0i}$, we get $\delta = \pi/2$ and the dipole resonates with the incident THz wave, and its vibrating amplitude reaches the maximum, which manifests as an absorption peak or a transmission dip in the fingerprint spectra of the sample molecule. When the difference between ω and ω_{0i} is large, the amplitude is very small, but as long as the external incident THz field exists, this vibration continuously living.

By Eq. (2), the electric field intensity of dipoles in the sample irradiated by the incident THz wave is obtained as follows:

$$\vec{E}(\omega) = \sum_{i=1}^{N}\left(-\frac{m_i}{e}\right)\left(\omega_{0i}^2-\omega^2-j\omega\gamma\right)\vec{r}_i(\omega) \tag{4}$$

where $\vec{r}_i(\omega)$ is the vibrating position vector of the ith dipole. $N = n\pi R^2 z$ is the number of dipoles. n, and z are the molecular number density, the thickness of the sample, respectively. R is the waist radius of the incident THz wave.

Thus, the radiation intensity of forced vibration produced by all of the molecular dipoles in the sample irradiated by the incident THz wave is obtained as follows:

$$I'(\omega) = \left|\vec{E}(\omega)\right|^2 = \left|\sum_{i=1}^{N}\left(-\frac{m_i}{e}\right)\left(\omega_{0i}^2-\omega^2-j\omega\gamma\right)\vec{r}_i(\omega)\right|^2 \tag{5}$$

By Eq. (5), $I'(\omega)$ carries the fingerprint frequencies of sample molecules. THz-TDS system is used to generate THz waves with wideband ω, and THz waves transmit through a sample by resonating with sample molecules, and then, spectral lines with characteristic absorption peaks or transmission dips are formed. Thus, ω_{0i}, the intrinsic central angular frequency of a sample molecule, is measured, realizing to analyze and identify configurations and physical properties of a sample molecule.

3. Results and discussions

In order to validate Eq. (5), we take the characteristic absorption spectra of water vapor as an example, because of its universal characteristics. Eq. (5) can be used to calculate line positions of the fingerprint spectra, i.e., absorption peaks of water vapor in the THz range. Then, the calculated results are compared with the experimental measurements. We set other parameters of water vapor in the discussion section, such as: $m_i = 3.0\times10^{-26}$ kg, $m = 1.0\times10^{-27}$ kg, $r_i = 0.956\times10^{-10}$ m, $n = 1.0\times10^{26}$ m^{-3}, $z = 1.0\times10^{3}$ m, $e = 1.60\times10^{-19}$ C, $c = 3.0\times10^{8}$ m/s, $R = 0.75\times10^{-3}$ m, and $\varepsilon_0 = 8.85\times10^{-12}$ F/m^2. We use MATLAB 2018b and ORIGIN 2018 tackled Eq. (5) and achieved these figures in the following sections.

3.1. Characteristic fingerprint spectra of water vapor

According to Refs. [5–9], there are some *recognized characteristic frequencies* (**RCF**) of absorption peaks in fingerprint spectra of water vapor as follows: 0.557, 0.752, 0.988, 1.097, 1.113, 1.163, 1.208, 1.229, and 1.412 THz. We think of these frequencies as known, and designate them as the values of $\omega_{0i}/(2\pi)$ respectively. Then, we substitute them into Eq. (5), one by one. Corresponding intensity-frequency graphs are plotted as Figs. 3, 5, and 6, respectively. We obtain the line positions of absorption peaks of water vapor from these graphs, and then compare them with the existed results in literature and the experimental measurements to verify the correctness of our expression Eq. (5).

In Ref. [6], dry air was as the reference and moist air as the sample, and their amplitude spectra are shown in Fig. 1(a). We select the

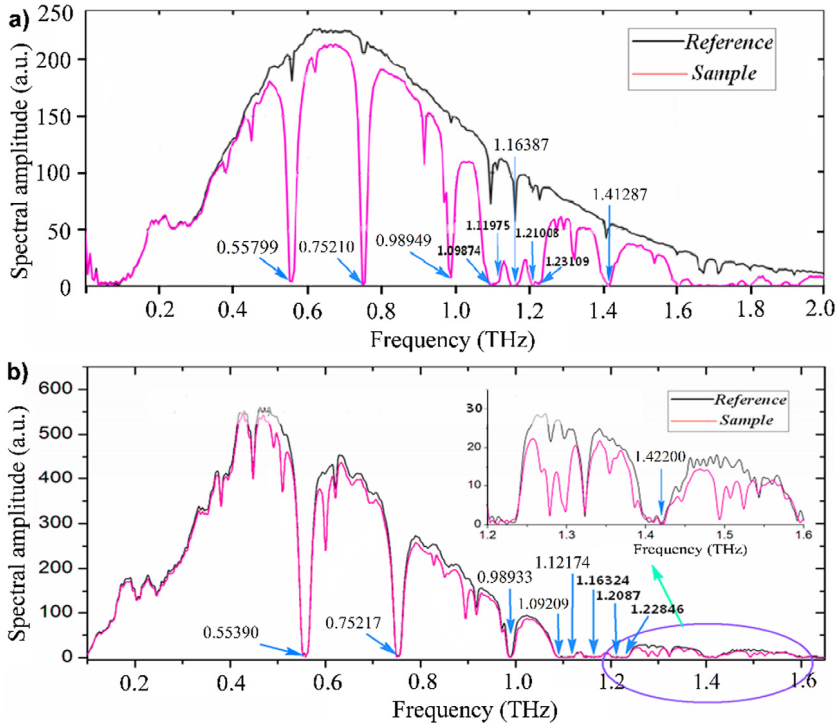

Fig. 1. Spectral amplitudes (upper curve, black) for the dry-air as THz reference pulse. Blue arrows indicate the absorption peaks of water vapor, values marked around them. (a) The amplitude spectrum (lower curve, red) for the humid-air as sample pulse (courtesy of [6]). (b) Signal (red curve) where D_2O liquid drops were introduced to a sample tube corresponding to a vapor concentration of 750 ppm and at relative humidity of 51% (courtesy of [7]). Inset shows the absorption peaks in the expanded higher frequency range. (For interpretation of the references to colour in this figure legend, the reader is referred to the web version of this article.)

sample's nine transmission dips at corresponding frequencies as follows, 0.55799, 0.75210, 0.98949, 1.09874, 1.11975, 1.16387, 1.21008, 1.23109, and 1.41287 THz. They correspond to absorption peaks of water vapor, respectively. We regard them as the comparison references to our results in this paper, and define them as Experimental Data 1. Relative errors between Experimental Data 1 and **RCF** are 0.18%, 0.02%, 0.16%, 0.16%, 0.61%, 0.08%, 0.18%, 0.17%, and 0.06%, respectively (Note: (0.55799 − 0.557)/0.557 = 0.18%, by analogy, later results and so on). Fig. 1(a) shows the absorptance corresponding to the first four is obviously higher than that of the latter five.

In Ref. [7], air spectra without D_2O droplets were as the reference, and air spectra with D_2O droplets were as the sample, and their amplitude spectra are shown in Fig. 1(b). Again, we select nine absorption peaks of water vapor at corresponding frequencies as follows, 0.55390, 0.75217, 0.98933, 1.09209, 1.12174, 1.16324, 1.20870, 1.22846, and 1.42200 THz. We also regard them as the comparison references to our results in this paper, and define them as Experimental Data 2. Relative errors between Experimental Data 2 and **RCF** are 0.56%, 0.03%, 0.14%, 0.45%, 0.79%, 0.02%, 0.06%, 0.05%, and 0.71%, respectively. Fig. 1(b) also shows the absorptance corresponding to the first four is significantly greater than that of the latter five.

From Fig. 2, all the line positions are not influenced by different relative humidity, and they all locate at their corresponding fixed positions, though their intensities showing a little difference. So, in the next sections, we ignore the influences of relative humidity, while calculating the line positions of the sample. Fig. 2 also shows a small amplitude range in the pink circle, which we will analyze in the latter section of this paper.

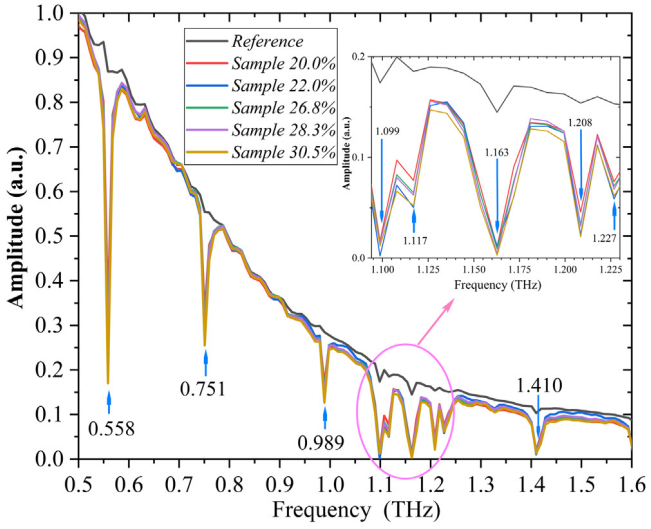

Fig. 2. Experimental measurements of absorption amplitudes of water vapor at different relative humidity: 20.0%, 22.0%, 26.8%, 28.3%, and 30.5%, respectively. Inset is the magnified graph of amplitudes in the range of 1.095–1.226 THz. Blue arrows indicate the absorption peaks of water vapor, values marked around them. (For interpretation of the references to colour in this figure legend, the reader is referred to the web version of this article.)

3.2. Forced radiation intensity $I'(\omega)$

Fig. 3 presents the trends of $I'(\omega)$ vs. frequencies of the incident THz wave. In 0–5.0 THz range, trends of the nine curves agree well with each other, which means $I'(\omega)$ increasing with the frequencies of the THz wave. However, in the range of 0–1.6 THz, $I'(\omega)$ of each curve decreases at first and then increases with frequencies, and the trends of the nine curves are just alike. While the nine curves decreasing nonlinearly during 0–0.566, 0–0.750, 0–0.990, 0–1.100, 0–1.120, 0–1.170, 0–1.201, 0–1.221, and 0–1.410 THz, respectively, and then increasing nonlinearly during 0.566–1.6, 0.750–1.6, 0.990–1.6, 1.100–1.6, 1.120–1.6, 1.170–1.6, 1.201–1.6, 1.221–1.6, and 1.410–1.6 THz, respectively, $I'(\omega)$ of each curve has a minimum value at the frequency

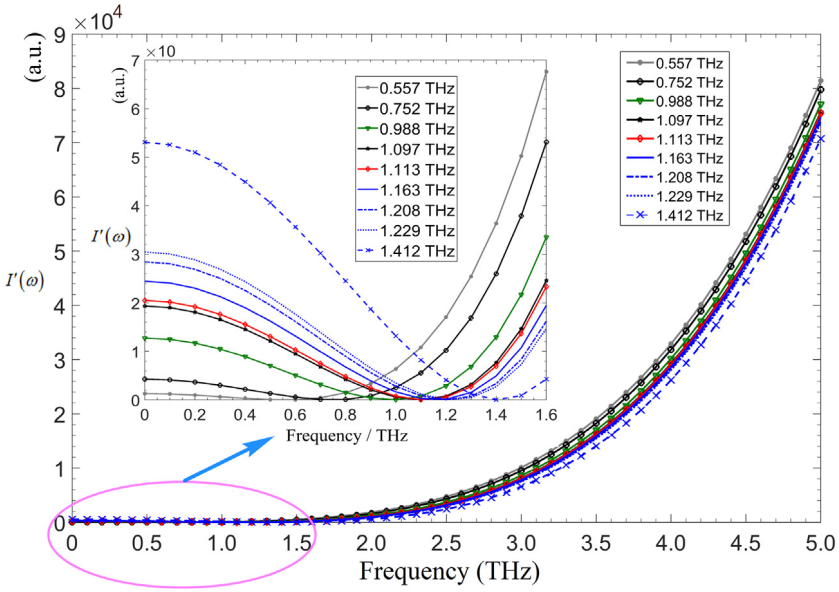

Fig. 3. (Color online) Plotted by Eq. (5). Relation curves for $I'(\omega)$ and frequencies of THz wave when $\omega_{0i}/(2\pi)$ = 0.557, 0.752, 0.988, 1.097, 1.113, 1.163, 1.208, 1.229, and 1.412 THz in Eq. (5), respectively. Inset is the magnified graph of $I'(\omega)$ in the range of 0–1.6 THz.

of 0.566, 0.750, 0.990, 1.100, 1.120, 1.170, 1.201, 1.221, and 1.410 THz, respectively.

In general, $A = 1–T–R$, where A is the absorptance of a sample, T is the transmissivity, and R is the reflectivity. The minimum value of transmission intensity means that the energies of the waves are both absorbed and reflected with the maximum value. However, the reflected wave is transmitted amongst the molecules, and finally, it becomes stray wave distracted in molecules and space. Thus, the minimum value of $I'(\omega)$ here means the absorption peak in fingerprint spectra while water vapor molecules absorb THz wave. Therefore, these frequencies corresponding to the 9 minimum values, listed above, are line positions of absorption peaks which calculated by Eq. (5) while taking the minimum values of $I'(\omega)$. We define them as the Calculation Results of this paper.

The line positions of counterpart characteristic absorption peaks can be pinpointed in the normal sequence in Fig. 3. We acquire these Calculation Results from the inset just right to be their corresponding calculated line positions. Relative errors between the Calculation Results and their counterpart RCF are as follows, 1.6%, 0.27%, 0.20%, 0.27%, 0.63%, 0.60%, 0.58%, 0.65%, and 0.14%, respectively. All of the errors are very low, and close to the errors in Fig. 1(a) and (b), which means that our calculated line positions of water vapor by Eq. (5) are perfectly consistent with experiments. The Calculation Results thus perfectly verify that Eq. (5) is right.

3.3. Comparison with DFT

To verify the superiority of Eq. (5), the line positions of water vapor obtained by Eq. (5) are compared with that of THz absorption peaks of water clusters simulated from DFT.

Fig. 4(a) shows the simulation results of amplitude spectra of THz wave absorbed by different number of water molecules according to DFT algorithm. Among them, 0.8596, 1.0743, 1.0759, 1.1033, 1.1134, 1.1845, 1.3255, and 1.4049 THz correspond to the absorption peaks of 8, 9, 12, 10, 6, 8, 13, and 11 water molecules, respectively. By comparison, it is found that they correspond to 0.752, 0.988, 1.097, 1.113, 1.163, 1.208, 1.229, and 1.412 THz in **RCF** of absorption peaks in the fingerprint spectra of water vapor, respectively. Other frequencies do not appear in the results of DFT.

A series of simulations were carried out with DFT to study the absorption spectra of various water clusters in the THz frequency range, where Gaussian-09 packets were used with B3LYP hybrid functional and 3-21G basis set. Based on the DFT simulation, we found that the water clusters with specific molecular numbers have the absorption peaks in the range of 0.5–1.45 THz as shown in Fig. 4(a). Typical configurations of water clusters with different molecular numbers corresponding to limited absorption peaks appeared in Fig. 4(a) are shown in Fig. 4(b)–(i), respectively.

As shown in Fig. 4(b)–(i), the molecules interact with each other in cluster via the way of hydrogen (H) bonds, and the vibration frequency of the H-bond network is indeed in the THz band, just as the description in Ref. [23]. After the process of configuration optimization, water molecules automatically form stable H-bonding structures to maintain the lowest total potential energy. The stable configurations of water clusters consisting of 6–13 molecules are shown in Fig. 4(b)–(i).

Experimental results show that water vapor has obvious absorption peaks in the frequency range of 0.5–1.6 THz [5–9]. Since each water cluster has different vibration degrees of freedom, each cluster has different vibration modes due to different H-bond networks. Only when the incident THz wave resonates with one of the vibration modes, the corresponding absorption peak is generated. The vibration modes and the construction of the clusters corresponding to the frequencies are also shown in Fig. 4(b)–(i), where each arrow represents the vibration direction of an atom, and all the arrows in a cluster form a specific vibration mode of the cluster. The collective effect of the specific vibration modes cause the corresponding amplitude of the absorption peaks to be large or small.

In contrast, the absorption peaks of water clusters which composed of 2, 3, 4, 5, 7 water molecules appear at 1.6–13 THz range, while that of a single water molecule locate at mid-infrared rather than at THz frequencies, as shown in Supplementary Material of this paper.

Table 1 shows the RCF, Experimental Data 1, Experimental Data 2, Simulation Results by DFT, Calculation Results by Eq. (5) in this paper, and the relative errors between them and RCF. As can be seen from Table 1, compared with the simulation results from DFT, the frequencies of absorption peaks calculated by Eq. (5), that is, the line positions, are even closer to the experimental results. Calculation Results obtained by Eq. (5) have the characteristics of small relative errors, accurate results, more comprehensive results, and convenient calculation. Thus, Eq. (5) is obviously superior to DFT algorithm in this case.

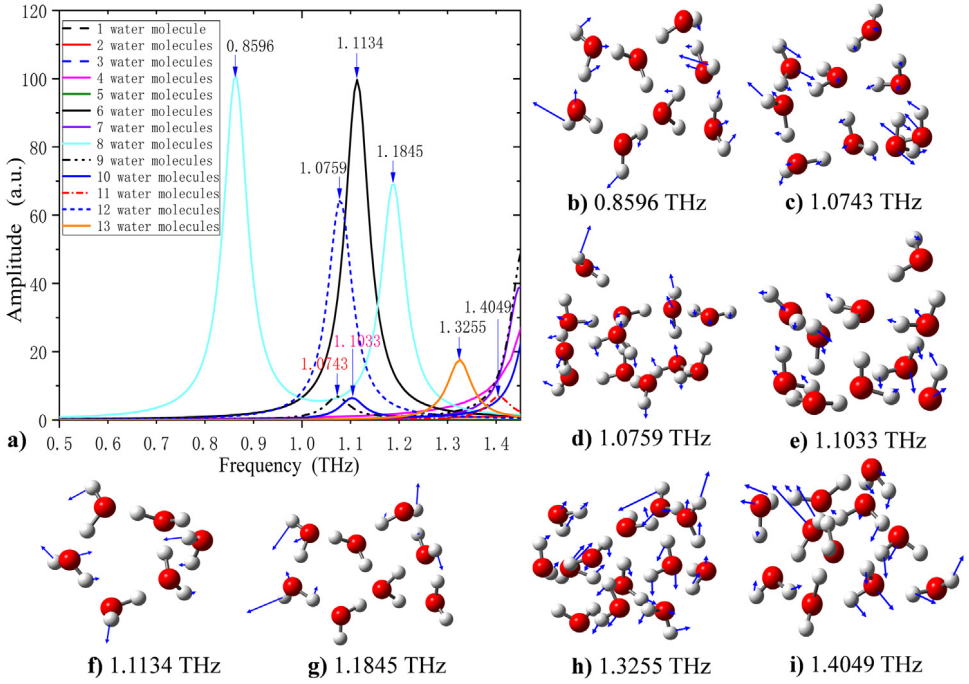

Fig. 4. DFT results. (a) Absorption amplitudes of water clusters composed of different numbers of molecules interacting with THz wave are simulated from DFT. Blue arrows indicate the absorption peaks of the water clusters, with frequencies marked around them. (b)–(i) Typical configurations of water clusters with different molecular numbers corresponding to respective absorption frequencies, where the red and gray balls represent the oxygen and hydrogen atoms, respectively. Blue arrows denote the directions of the atoms' vibration, and the length of each arrow represents the magnitude of the amplitude. (For interpretation of the references to colour in this figure legend, the reader is referred to the web version of this article.)

Table 1
Comparisons among the results of experimental measurements, the simulation results by DFT, and the results calculated by our expression Eq. (5).

Items	Values								
RCF (THz)	0.557	0.752	0.988	1.097	1.113	1.163	1.208	1.229	1.412
Experimental Data 1 (THz)	0.55799	0.75210	0.98949	1.09874	1.11975	1.16387	1.21008	1.23109	1.41287
Relative errors to RCF (%)	0.18	0.02	0.16	0.16	0.61	0.08	0.18	0.17	0.06
Experimental Data 2 (THz)	0.55390	0.75217	0.98933	1.09209	1.12174	1.16324	1.20870	1.22846	1.42200
Relative errors to RCF (%)	0.56	0.03	0.14	0.45	0.79	0.02	0.06	0.05	0.71
Simulation results by DFT (THz)	/	0.8596	1.0743	1.0759	1.1033	1.1134	1.1845	1.3255	1.4049
Relative errors to RCF (%)	/	14	8.8	2.0	0.87	4.3	2.0	7.9	0.50
Calculation Results by Eq. (5) in this paper (THz)	0.566	0.750	0.990	1.100	1.120	1.170	1.201	1.221	1.410
Relative errors to RCF (%)	1.6	0.27	0.20	0.27	0.63	0.60	0.58	0.65	0.14

3.4. The total forced radiation intensity $I'tol$

To further investigate the meaning of Eq. (5), we sum all the nine intensities of water vapor and get the function, $I'tol$, the total forced radiation intensity of all the molecular dipoles in the sample irradiated by the incident THz wave, as shown in Fig. 5. In the range of 0–5.0 THz, $I'tol$ increases with the increasing frequencies of the THz wave all the way. However, in the range of 0–1.6 THz, $I'tol$ fluctuates with the frequencies as shown in the inset of Fig. 5. There exists an absorption peak at 1.110 THz, while $I'tol$ decreases in the range of 0–1.110 THz and increases from 1.110 THz on. In Fig. 6, we compare the differences and relations between $I'(\omega)$ and $I'tol$. We find that the magnitude of $I'tol$ at 1.110 THz is obviously greater than that of any of the nine frequencies in the inset of Fig. 6, which means that there exists a superposition. Nevertheless, seen from the entire band of 0–5 THz in Figs. 5 and 6, the intensity at 1.110 THz is so small that it can be negligible.

Then, we search in Figs. 1 and 2, and sure enough to find that there indeed exists an overlapped absorption band at 1.09874, 1.11975, 1.16387, 1.21008, and 1.23109 THz in Fig. 1(a), and 1.09209, 1.12174, 1.16324, 1.20870, and 1.22846 THz in Fig. 1(b), and 1.099, 1.117, 1.163, 1.208, and 1.227 THz in Fig. 2, respectively. Moreover, their amplitudes are all obviously very small. These appearances are consistent with those obtained in Figs. 5 and 6, which further prove that the line positions and intensities of the absorption peaks calculated by Eq. (5) are credible.

3.5. Coherent superposition with $I'tol$

One might wonder why the minimum value of $I'tol$ is at 1.110 THz but not at anywhere else in Figs. 5 and 6, and why its amplitude and intensity are so small here. The reasons are that the forced vibrations of molecular dipoles form an approximate coherent superposition here. As we know, three conditions shown as follows must be met simultaneously when coherent superposition occurs. (1) The frequencies of the superimposed waves are equal. (2) The vibration directions of the superimposed waves are parallel. (3) The phase difference of the superimposed waves is constant. We call these three items as coherent conditions [24–26]. In general, coherent conditions result in two effects: one is destruction when the phase difference is $(2k+1)\pi$, and the other is construction when the phase difference is $2k\pi$, where $k = 0, 1, 2, 3, \ldots$.

By using Eq. (5), Figs. 6 and 7, we can explain this effect resorting to coherent conditions as follows. (1) Five of the nine **RCF**, i.e. 1.097, 1.113, 1.163, 1.208, and 1.229 THz, are close to each other and nearly

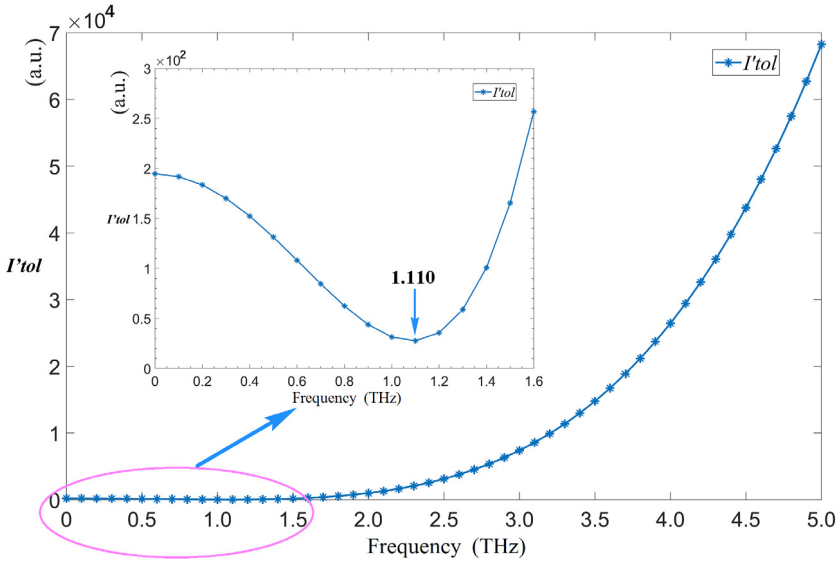

Fig. 5. (Color online) Plotted by Eq. (5). Relation curve for $I'tol$ and frequencies of the THz wave. Inset is the magnified graph of $I'tol$ in the range of 0–1.6 THz. There shows an absorption peak at 1.110 THz.

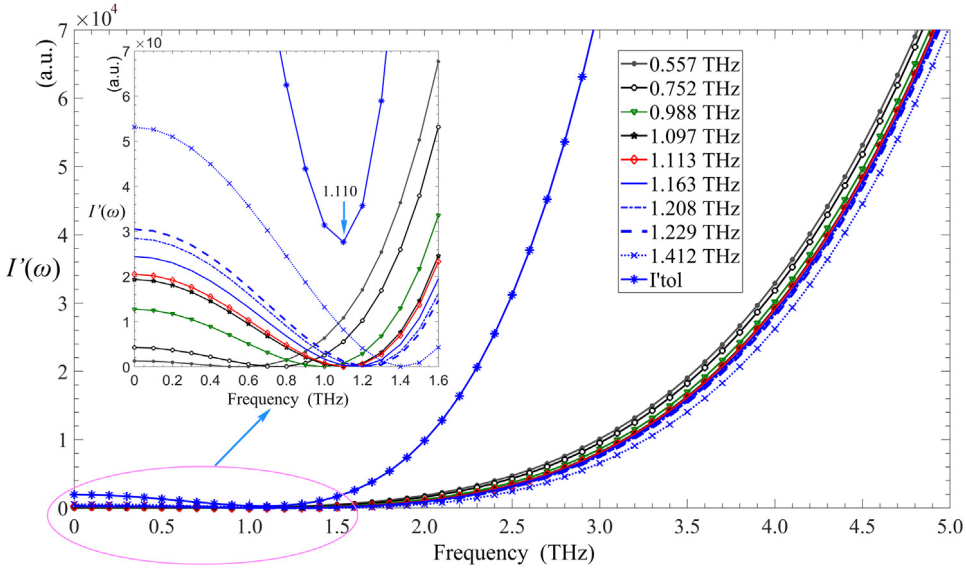

Fig. 6. (Color online) Plotted by Eq. (5). Relation curves for $I'(\omega)$, $I'tol$, and frequencies of the THz wave. Left inset is magnified graphs of $I'(\omega)$ and $I'tol$ in the range of 0–1.6 THz.

around 1.110 THz. So the first item of the coherent conditions is almost met. (2) The polarization direction of the THz waves transmitted from the sample is consistent with that of the dipoles when resonating. So the second item of the coherent conditions is met. (3) Transmitted THz waves corresponding to these five frequencies are modulated by dipoles' motion, and their phase differences are constant because usually we do not modulate transmitted waves at free space. According to Eq. (3), we sure enough to get their phase difference being almost π at 1.110 THz, as Fig. 7 shows. So the third item of the coherent conditions is met. To sum up, these three above-mentioned items result in an approximately destructive coherent superposition in transmitted THz waves, and forming this very small amplitude at 1.110 THz. However, there are big differences between other frequencies and they cannot be coherent because of hardly satisfying the coherent conditions, just right as the results we get from Figs. 1 and 2. Therefore, we can analyze the effect of coherent superposition using Eq. (5) by calculating absorption intensities.

4. Conclusions

In closing, for predicting the THz-fingerprint peaks of samples, we propose a quantitative expression based on the classical forced vibration model of dipoles, i.e. the forced radiation intensity of molecular electric dipoles. Because of water vapor's universal characteristics, we verified our expression by 9 recognized characteristic frequencies of water vapor in the THz band. Both the line positions and intensities of absorption peaks calculated by our expression are perfectly consistent with the experimental measurements. Compared with the results of different number of water clusters simulated from DFT, our expression is obviously superior to the DFT algorithm in this example. Furthermore, specially, our expression also supports the theory of coherent superposition, which can be used for exactly analyzing the generation mechanism of molecular fingerprint spectroscopy at THz frequencies. As far as we know, very few studies have been done on the coherent superposition in the current field of THz absorption spectroscopy, while our expression demonstrates a perfect performance on it. As to other

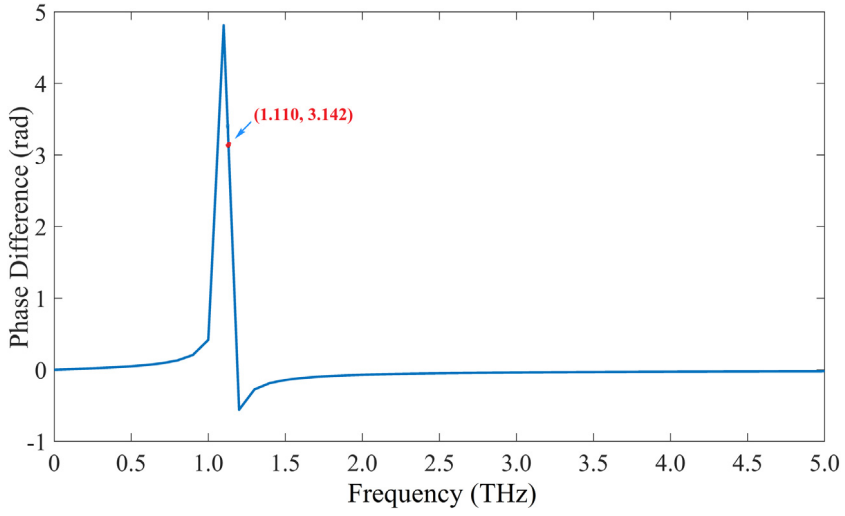

Fig. 7. (Color online) Plotted by Eq. (3). Phase difference between transmitted THz waves modulated by dipoles' motion. A red dot is marked on the curve, accompanied by its coordinate value, which manifests that while at 1.110 THz, the phase difference is almost π.

samples, such as organic molecules and solid plasmonic samples, we will continue to verify and predict their line positions and coherent superposition by our expression.

Acknowledgments

This work is financially supported by the Natural Science Foundation of China [grant numbers 61722111, 11904231, 61671302]; Shanghai Pujiang Program, China [grant number 17PJD028]; the 111 Project [grant number D18014]; Shanghai Sailing Program [grant number 19YF1434100]; Zhejiang Agriculture and Forestry University Project [grant number 201311012850]; Zhejiang Science and Technology Department Project [grant number 2017C37015]; the Shuguang Program [grant number 18SG44].

Appendix A. Supplementary data

Supplementary material related to this article can be found online at https://doi.org/10.1016/j.optcom.2019.124848.

References

[1] M.D. King, W.D. Buchanan, T.M. Korter, Investigating the anharmonicity of lattice vibrations in water-containing molecular crystals through the Terahertz spectroscopy of L-Serine Monohydrate, J. Phys. Chem. A 114 (35) (2010) 9570–9578.
[2] G.A. Melentev, V.A. Shalygin, L.E. Vorobjev, et al., Interaction of surface plasmon polaritons in heavily doped GaN microstructures with terahertz radiation, J. Appl. Phys. 119 (9) (2016) 12.
[3] J.J. Ma, F. Vorrius, L. Lamb, et al., Comparison of experimental and theoretical determined Terahertz Attenuation in controlled rain, J. Infrared Millim. Te. 36 (12) (2015) 1195–1202.
[4] P. Babilotte, L.H. Coudert, F. Billard, et al., Experimental and theoretical study of free induction decay of water molecules induced by terahertz laser pulses, Phys. Rev. A 95 (4) (2017) 6.
[5] M. Van Exter, C. Fattinger, D. Grischkowsky, Terahertz time-domain spectroscopy of water vapor, Opt. Lett. 14 (20) (1989) 1128.
[6] Y. Yang, A. Shutler, D. Grischkowsky, Measurement of the transmission of the atmosphere from 0.2 to 2 THz, Opt. Express 19 (9) (2011) 8830–8838.
[7] J.S. Melinger, Y. Yang, M. Mandehgar, et al., THz detection of small molecule vapors in the atmospheric transmission windows, Opt. Express 20 (6) (2012) 6788–6807.
[8] Y. Huang, P. Sun, Z. Zhang, et al., Numerical method based on transfer function for eliminating water vapor noise from terahertz spectra, Appl. Opt. 56 (20) (2017) 5698–5704.
[9] Y. Yang, M. Mandehgar, D. Grischkowsky, Determination of the water vapor continuum absorption by THz-TDS and molecular response theory, Opt. Express 22 (4) (2014) 4388–4403.
[10] L. Chen, D. Liao, X. Guo, et al., Terahertz time-domain spectroscopy and micro-cavity components for probing samples: a review, Front. Inform. Technol. Electron. Eng. 20 (5) (2019) 591–607.
[11] H. Hu, X. Yang, F. Zhai, et al., Far-field nanoscale infrared spectroscopy of vibrational fingerprints of molecules with graphene plasmons, Nature Commun. 7 (12334) (2016) 12334.
[12] Y. Su, X. Zheng, X. Deng, Terahertz spectrum analysis based on empirical mode decomposition, J. Infrared Millim. Te. 38 (8) (2017) 972–979.
[13] A.E. Siegman, Lasers, University Science Books, 1986.
[14] A. Carpinteri, G. Lacidogna, G. Piana, et al., Terahertz mechanical vibrations in lysozyme: Raman spectroscopy vs modal analysis, J. Mol. Struct. 1139 (2017) 222–230.
[15] M. Birk, G. Wagner, J. Loos, et al., Accurate line intensities for water transitions in the infrared: Comparison of theory and experiment, J. Quant. Spectrosc. Radiat. Transfer 203 (SI) (2017) 88–102.
[16] O.L. Polyansky, A.A. Kyuberis, L. Lodi, et al., Exomol molecular line lists XIX: high-accuracy computed hot line lists for (H_2O)-O-18 and (H_2O)-O-17, Mon. Not. R. Astron. Soc. 466 (2) (2017) 1363–1371.
[17] L. Lodi, J. Tennyson, Line lists for (H_2O)-O-18 and (H_2O)-O-17 based on empirical line positions and ab initio intensities, J. Quant. Spectrosc. Radiat. Transfer 113 (11SI) (2012) 850–858.
[18] L. Chen, Y. Wei, X. Zang, et al., Excitation of dark multipolar plasmonic resonances at terahertz frequencies, Sci. Rep. -Uk 6 (1) (2016) 22027.
[19] Y. Zhou, E. Y, X. Xu, et al., Angular dependent anisotropic terahertz response of vertically aligned multi-walled carbon nanotube arrays with spatial dispersion, Sci. Rep. -Uk 6 (2016).
[20] H. Yao, S. Zhong, Frequency-dependent circular-polarization of terahertz chiral spoof surface plasmon polariton on helically grooved metallic wire, Opt. Commun. 354 (2015) 401–406.
[21] K.N. Egodapitiya, S. Li, R.R. Jones, Terahertz-induced field-free orientation of rotationally excited molecules, Phys. Rev. Lett. 112 (10) (2014).
[22] F. Carreno, M.A. Anton, S. Melle, et al., Plasmon-enhanced terahertz emission in self-assembled quantum dots by femtosecond pulses, J. Appl. Phys. 115 (6) (2014).
[23] D. Laage, T. Elsaesser, J.T. Hynes, Water dynamics in the hydration shells of Biomolecules, Chem. Rev. 117 (16SI) (2017) 10694–10725.
[24] C. Rosenbury, Y. Gu, G. Gbur, Phase singularities, correlation singularities, and conditions for complete destructive interference, J. Opt. Soc. Am. A 29 (4) (2012) 410–416.
[25] D. Kong, X. Wu, B. Wang, et al., High resolution continuous wave terahertz spectroscopy on solid-state samples with coherent detection, Opt. Express 26 (14) (2018) 17964–17976.
[26] J. Saisut, S. Rimjaem, C. Thongbai, A THz spectroscopy system based on coherent radiation from ultrashort electron bunches, J. Infrared Millim. Te. 39 (7) (2018) 681–700.